Long-term preservation effects on biological properties of acellular placental sponge patches

Materials Science & Engineering C 121 (2021) 111814

Contents lists available at ScienceDirect

Materials Science & Engineering C

journal homepage: www.elsevier.com/locate/msec

Long-term preservation effects on biological properties of acellular placental sponge patches

Fatemeh Asgari [a,b,1], Sadjad Khosravimelal [c,d,e,1], Morteza Koruji [a,b], Zahra Aliakbar Ahovan [f], Ali Shirani [c,e], Ali Hashemi [f], Hatef Ghasemi Hamidabadi [g,h], Narendra Pal Singh Chauhan [i], Lorenzo Moroni [j], Rui L. Reis [k], Subhas C. Kundu [k,*], Mazaher Gholipourmalekabadi [c,e,d,**]

[a] Stem cell and Regenerative Medicine Research Center, Iran University of Medical Sciences, Tehran, Iran
[b] Department of Anatomical Sciences, School of Medicine, Iran University of Medical Sciences, Tehran, Iran
[c] Cellular and Molecular Research Center, Iran University of Medical Sciences, Tehran, Iran
[d] Department of Medical Biotechnology, Faculty of Allied Medicine, Iran University of Medical Sciences, Tehran, Iran
[e] Department of Tissue Engineering & Regenerative Medicine, Faculty of Advanced Technologies in Medicine, Iran University of Medical Sciences, Tehran, Iran
[f] Department of Microbiology, School of Medicine, Shahid Beheshti University of Medical Sciences, Tehran, Iran
[g] Immunogenetic Research Center, Department of Anatomy & Cell Biology, Faculty of Medicine, Mazandaran University of Medical Sciences, Sari, Iran
[h] Department of Anatomy & Cell Biology, Faculty of Medicine, Mazandaran University of Medical Sciences, Sari, Iran
[i] Department of Chemistry, Faculty of Science, Bhupal Nobles' University, Udaipur, Rajasthan, India
[j] Complex Tissue Regeneration Department, Maastricht University, MERLN Institute for Technology-Inspired Regenerative Medicine, Universiteitssingel 40, 6229 ER Maastricht, the Netherlands
[k] 3Bs Research Group, I3Bs - Research Institute on Biomaterials, Biodegradable and Biomimetics, Headquarters of the European Institute of Excellence on Tissue Engineering and Regenerative Medicine, University of Minho, AvePark, Guimaraes, Portugal

ARTICLE INFO

Keywords:
Placenta
Decellularization
Preservation
Angiogenesis
Antibacterial

ABSTRACT

Decellularization, preservation protocol and storage time influence the biomechanical and biological properties of allografts and xenografts. Here, we examined the consequences of storage time on the antibacterial, angiogenic and biocompatibility properties of the decellularized placental sponge (DPS) *in vitro* and *in vivo*. The DPS samples were preserved for one, three and six months at −20 °C. The decellularized scaffolds showed uniform morphology with interconnected pores compared with not decellularized sponges. Storage time did not interfere with collagen and vascular endothelial growth factor contents, and cytobiocompatibility for Hu02 fibroblast cells. Chorioallantoic membrane assay and subcutaneous implantation indicated a decreased new vessel formation and neovascularization in six months DPS sample compared with other experimental groups. The number of $CD4^+$ and $CD68^+$ cells infiltrated into the six months DPS on the implanted site showed a significant increase compared with one and three months sponges. The antibacterial activities and angiogenic properties of the DPS decreased over storage time. Three months preservation at −20 °C is suggested as the optimal storage period to retain its antibacterial activity and high stimulation of new vessel formation. This storage protocol could be considered for preservation of similar decellularized placenta-derived products with the aim of retaining their biological properties.

1. Introduction

Extracellular matrix (ECM) is considered as a biologically attractive material in tissue engineering and regenerative medicine [1]. ECM provides a wide range of biological cues for cell migration, proliferation and conduction/promoting differentiation [2]. It also contains different growth factors, proteins, glycosaminoglycans, hyaluronic acid and other substances [3]. To date, several ECM-based tissue engineering scaffolds

* Corresponding author.
** Correspondence to: M. Gholipourmalekabadi, Department of Tissue Engineering & Regenerative Medicine, Faculty of Advanced Technologies in Medicine, Iran University of Medical Sciences, Tehran, Iran.
E-mail addresses: kundu@i3bs.uminho.pt (S.C. Kundu), mazaher.gholipour@iums.ac.ir, mazaher.gholipour@gmail.com (M. Gholipourmalekabadi).
[1] The authors equally contributed to this work.

https://doi.org/10.1016/j.msec.2020.111814
Received 8 September 2020; Received in revised form 18 November 2020; Accepted 14 December 2020
Available online 24 December 2020

are developed from natural tissues such as placenta, heart, lung and skin. Some of the products are now in the market [4].

ECM-based scaffolds are excellent substrates for multiple cellular functions like migration and propagation, reducing scar formation and minimizing immunological reactions [5,6]. Graft rejection by the host immune system is one of the important issues, which need to be considered during preparation of such biological scaffolds. In this regard, the decellularization process is applied to remove the host cells with minimal damages to the ECM contents, and needs to minimize subsequently the risk of graft rejection [7]. Generally, decellularization protocols are divided as chemical, mechanical and enzymatic strategies, or a combination of them [8]. Decellularization process remarkably alters the composition, biomechanical and biological properties of the decellularized ECM. The severity of these damages to ECM depends on the denuding agents used during decellularization [9,10]. Therefore, it is important to optimize a decellularization process with minimal negative effects on ECM contents, especially on growth factors, and full removal of cells or cells' fragments. Sodium dodecyl sulfate (SDS) is the most effective ionic detergent for tissue decellularization [11]. Despite its well-established efficiency, SDS shows some degrees of negative effects on natural tissues, depending on its concentration and incubation time. Thus, it is very important to optimize its concentration and treatment time for each tissue, or to blend SDS with some nonionic detergent like Triton to minimize its destructive effects. Triton alone is able to successfully remove the cells from some of the soft tissues. In addition, treatment of tissue with Triton after SDS shows to be helpful in both decellularization and removal of residual of SDS [12,13]. The preservation condition is also very critical, which affects remarkably the quality of the ECM based scaffolds. It is shown that preservation methods and storage time can remarkably influence the biomechanical and biophysical properties of the decellularized tissues [14–16].The decellularized tissues can be stored through the different preservation methods until experimental or clinical uses. Freeze-drying and cryopreservation are two common preservation methods for long-time preservation of tissue-derived tissue engineering products [14,15].

The effects of preservation methods and incubation time on some of the biological materials such as decellularized amniotic membranes are investigated [17–20]. For example, Tehrani et al. [20] and Niknejad et al. [18] have studied the effects of preservation methods on antibacterial properties and also the substrate characteristics of human amniotic membrane. Johnson et al. [17] have also examined the consequences of different preservation methods on the integrity and functionality of human amniotic membranes. The main aim of our current study is to determine the impacts of preservation processing and storage time on the biological characteristics of the decellularized placental sponge patches.

Placenta is a multiplex organ equipped with ample vascular networks that enable the exchange of physiological requirements between the fetus and maternal circulatory systems [9,21]. Placenta contains an ECM with basement membrane proteins, proteoglycans, collagen types I, III, IV and XVII, elastin, laminin and fibronectin [5,22] and several growth factors like insulin-like growth factors 1 and 2, epidermal growth factor, platelet-derived growth factor, fibroblast growth factors, vascular endothelial growth factor (VEGF) and transforming growth factor-β [23]. These compositions endow biocompatibility, anti-inflammatory, antibacterial, anti-scarring and angiogenic properties to the placenta and make it an excellent allograft biological source for biomedical applications [22]. In this study, we evaluate the effects of decellularization method and storage duration on the angiogenic property, antibacterial activity (against both standard strain and multidrug resistant clinical isolates) and biocompatibility of the acellular placental sponge patches *in vitro* and *in vivo*. Our results indicate that the preservation and storage time are variables that need to be considered for future study design and production of human placenta-based tissue engineered matrices.

2. Materials and methods

The summary of the current study design is illustrated in Fig. 1. The placenta tissue was decellularized and then freeze dried to fabricate the decellularized placental sponge (DPS). The sponges were preserved for different storage times of one, three and six months at −20 °C. The effects of storage time on morphology, ECM content, biocompatibility, angiogenic properties and antibacterial activity against three standard strain bacteria and three multidrug-resistant clinical isolated bacteria were examined *in vitro* and *in vivo* and were compared with the control group (the native placenta homogenized and washed for 8 consecutive days).

2.1. Ethics statement

All human sample collections and animal studies were approved by Iran University of Medical Sciences ethical committee's under approval ID of "IR.IUMS.REC.1398.767".

2.2. Tissue collection

Human placentas were obtained from the consenting mothers after their cesarean section deliveries, according to the World Medical Association Declaration of Helsinki [24]. All the candidates were screened for the possibility of infectious diseases such as human immunodeficiency virus type II, syphilis, hepatitis virus types B and C, gonorrhea, toxoplasmosis, and cytomegalovirus.

2.3. Decellularization procedures

The decellularization procedure was conducted in accordance with a previously developed method by Choi et al. [9,22]. Briefly, the placentas were washed with distilled water to remove any blood clots. The amniotic and chorionic membranes and umbilical cord were completely separated and the remained tissue was cut into small slices. Then, they were homogenized for 10 min on the ice using a blender. The homogenized placenta was suspended in 0.5% Triton™ X-100 and 0.5% sodium dodecyl sulfate (SDS) for 30 min. The samples were washed with phosphate-buffered saline (PBS) (all obtained from Sigma-Aldrich, MO, USA) and then centrifuged several times, each round at 1500 rpm, 4 °C for 10 min. The decellularized tissue was gently poured into a 24-well cell culture plate, and was immediately transferred to-80 °C for 24 h. The samples were freeze-dried (Alpha 1–2 LD plus, Christ, Germany) for 24 h. The decellularized placental sponges (DPS) were divided into three experimental groups according to the storage duration as follows: storage at −20 °C for one, three and six months (1 M, 3 M and 6 M, respectively).

2.4. Placenta characterizations

2.4.1. DNA content

DNA of the samples was extracted using a QiaAmp mini kit (Qiagen, USA). Total DNA content was (ng/mg) measured using a NanoDrop spectrophotometer (2000C, Thermo Fisher Scientific, USA) and was compared between one, three and six months DPS samples.

2.4.2. H&E staining

The samples were fixed with 10% formalin, dehydrated through a graded ethanol series, embedded in paraffin, and cut into 5 μm thickness slices by a microtome (Thermo Fisher Scientific, Waltham, Massachusetts, USA). The successful removal of the cells from placenta after decellularization process was confirmed with hematoxylin and eosin (H&E) staining.

2.4.3. Masson's trichrome (MT) staining

The slides were also stained with Masson's trichrome (MT) to

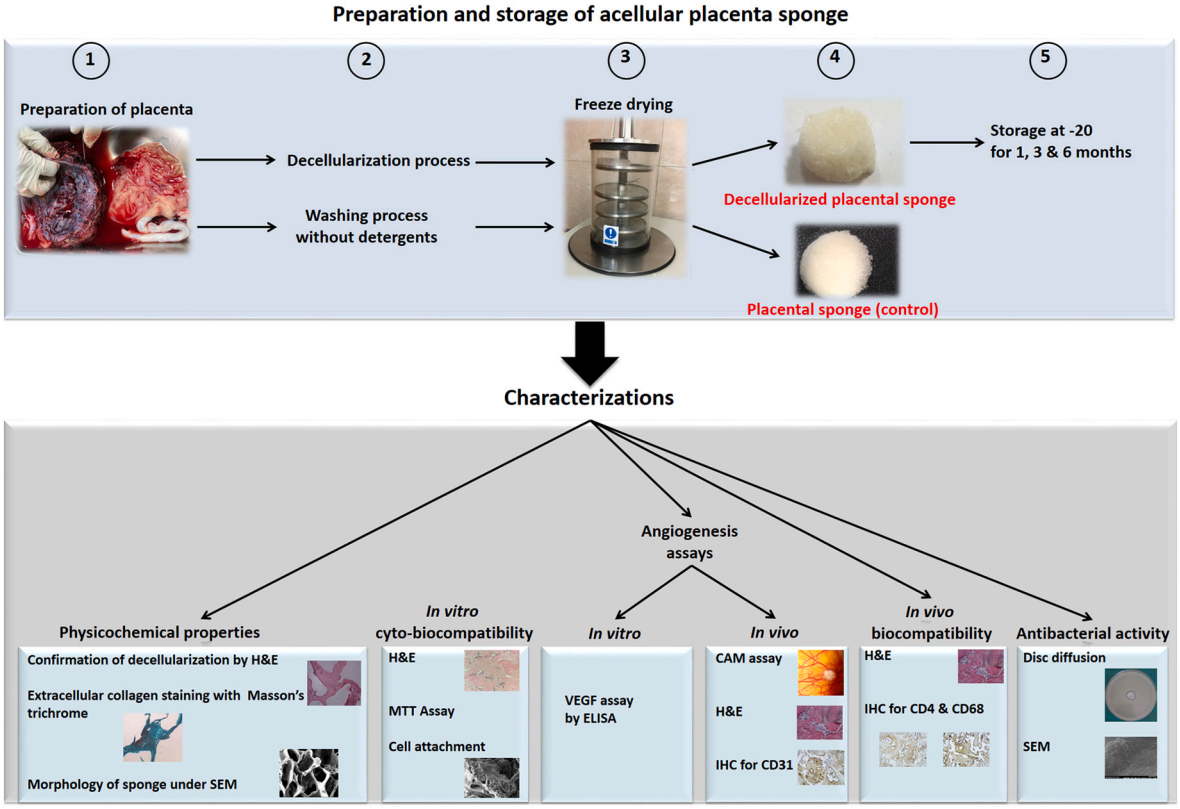

Fig. 1. Summary of the current designed study plan. The decellularized placental sponges were fabricated and preserved at −20 °C for one, three and six months. The effects of storage time on physicochemical, biocompatibility, angiogenic and antibacterial activities of the placental sponges were evaluated *in vitro* and *in vivo* and compared with the control (native placental tissues washed for 8 days after homogenization).

visualize collagen fibers. The stained sections were viewed under a light microscope (Olympus Corporation, Shinjuku, Tokyo, Japan).

2.4.4. Scanning electron microscope (SEM)

The samples were sputter coated with gold, then subjected to taking micrographs under scanning electron microscope (SEM, AIS2100; Seron Technology, Gyeonggi-do, South Korea).

2.5. In vitro cyto-biocompatibility assay

In vitro cyto-biocompatibilities of the sponges for Hu02 human foreskin fibroblast cells (purchased from Iranian Biological Resource Center, Tehran, Iran) were assessed by H&E staining, MTT assay and the cell morphology under SEM. The cells were cultured on 1 M, 3 M and 6 M DPSs in Dulbecco's Modified Eagle Medium (DMEM) supplemented with 10% fetal bovine serum (FBS), nystatin, 1% penicillin/streptomycin (pen/strep), amphotericin B, 2 mM Glutamax, 1% non-essential amino acids and 1 mM L-glutamine (all from Gibco, Carlsbad, CA, USA). They were incubated under the standard sterile condition having 95% humidity and 5% CO_2 at 37 °C for different time intervals, depending upon the assays.

2.5.1. H&E staining

A density of 5×10^4 cells·ml^{-1} were seeded on one, three and six months stored DPS scaffolds and were incubated for 7 days in a 24-well cell culture plate. The cell/sponge constructs were then stained with H&E, as described above, and observed under the light microscope.

2.5.2. Cell viability

MTT assay was performed according to our previously published protocol with minor modifications [25]. In brief, 2×10^4 cells/ml were cultured on the DPSs and incubated for 1, 3 and 7 days in 96-well cell culture plates. After each time interval, the cell-sponge constructs were washed with PBS, and treated with tetrazolium salt (*MTT* (3-(4,5-dimethylthiazol-2-yl)-2,5-diphenyltetrazolium bromide), Sigma-Aldrich, MO, USA) at 37 °C for 3 h. The formazan crystals formed in mitochondria of living cells were dissolved in dimethyl sulfoxide (DMSO, Sigma-Aldrich, MO, USA) in a dark chamber. The optical density was measured using a microplate-reader (DANA, DA3200) at 570 nm. The cells cultured on the plastic surface of the cell culture plate without DPS served as control, and considered as 100% cell viability.

2.5.3. SEM

The morphology of the cells grown on the DPSs was observed under SEM. In brief, a density of 5×10^4 Hu02 cells was seeded on the sponges (1 × 1 cm) and was incubated for 7 days in 5% CO_2 at 37 °C. The cells-DPS constructs were fixed with 2.5% glutaraldehyde, dehydrated through a graded series of ethanol and dried under vacuum. The samples were sputter-coated with gold and observed under SEM (AIS2100; Seron Technology, South Korea) at an accelerating voltage of 15 kV.

2.6. Angiogenesis assay

2.6.1. In vitro VEGF assay

Vascular endothelial growth factor (VEGF) concentrations in different groups of DPSs (1, 3 and 6 M) were measured using a commercially available enzyme-linked immunosorbent assay (ELISA) kit, according to the manufacturer's instructions, and then read by an ELx800 absorbance microplate reader at 450 nm. The concentration of VEGF in DPSs was compared with control placental sponge (without decellularization).

2.6.2. In vivo angiogenesis assay

2.6.2.1. Chick chorioallantoic membrane (CAM) assay. Nine fertile eggs (Hy-Line Brown) were divided into three the decellularized placental sponge (DPS) groups (n = 3) of one, three and six months (coded as 1 M, 3 M and 6 M, respectively). For Chick chorioallantoic Membrane (CAM) assay, the eggshell was cut and the DPS samples were positioned on the egg chorion-allantois membrane surfaces. The eggs were incubated at 37.5 °C, and 40 to 60 percent humidity using an incubator (Easy Jik, Genesis model, Iran). On day three, 3 of albumin was aspirated from the eggs by a 5 ml-syringe. The scaffolds were located into the chorion-allantois membrane on the 8th day. On the 14th day of incubation, the CAM was imaged using a stereomicroscope (ZSM-1001, SA Iran co., Iran) attached to a digital camera (Nikon D3200, Thailand). The total vascular junction points and vessel percentage area (area of the vessels relative to the total area of the image) were analyzed using ImageJ software (version 1.8.0_112, Vessel Analysis plugin).

2.6.2.2. Histological evaluations (H&E and immunohistochemistry (IHC)). For *in vivo* angiogenesis investigations, the DPS scaffolds (1, 3 and 6 M) were subcutaneously implanted in NMRI male mice (n = 6 for each group). The implanted sites of each group were collected at one and four weeks post-implantation and were stained with H&E and IHC for histological evaluations and CD31 positive cells, respectively. For IHC staining, after each time intervals, animals were sacrificed by CO_2 asphyxiation, and the samples were collected from the implanted area. The tissues were fixed with 10% formalin, dehydrated through a graded series of ethanol (up to 100%), and then carried out paraffin embedding for histological investigations. The paraffin blocks were sectioned at 6 μm. The slides were treated with CD31 primary antibody, and visualized with horseradish peroxidase (HRP)-conjugated secondary antibody (both antibodies purchased from human monoclonal IgG, Santa Cruz Biotechnology, USA). Images were captured on ten random fields by a light microscope and analyzed by ImageJ software (version 1.8.0_112, Vessel Analysis plugin).

2.7. In vivo biocompatibility

For evaluation of *in vivo* biocompatibility, the subcutaneous implanted DPS scaffolds were stained with H&E and IHC at one and four weeks after implantation. For IHC staining, the slides were treated with CD4 (for T helper cells) and CD68 (for macrophages) primary antibodies, and were visualized with HRP-conjugated secondary antibody (all human monoclonal IgG antibodies purchased from Santa Cruz Biotechnology, USA). The staining was performed according to the manufacturer's instructions (n = 3 per condition, from all treated placentas). Ten random fields were chosen and imaging was conducted under a light microscope. The images were analyzed using ImageJ software (version 1.8.0_112, Vessel Analysis plugin).

2.8. Antibacterial assay

2.8.1. Disk diffusion assay

Antibacterial activities of DPS scaffolds (1, 3 and 6 M) against standard strains and multidrug resistant (MDR) clinical isolates were determined by disk diffusion assay. The observations of the bacteria grown on the scaffolds were carried out under SEM.

Antibacterial activities of the DPS disks against three bacterial standard strains of *Staphylococcus aureus* (ATCC 25923), *Escherichia coli* (ATCC 25922) and *Pseudomonas aeruginosa* (PAO1), and three MDR clinical isolates of *S. aureus* (MDR 50), *E. coli* (MDR 50) and *P. aeruginosa* (MDR 50) were determined by Bauer-Kirby disk diffusion method, according to clinical and laboratory standards institute (CLSI) guidelines [26]. In brief, 100 μl of 0.5 McFarland (1.5×10^8 CFU/ml) bacterial suspensions were cultured on Mueller-Hinton Agar (MHA) plates. Then, the DPS disks (0.5 cm in diameter) were placed on the center of each plate, and were incubated at 37 °C for 24 h. The bacterial growth inhibition zone was measured using a ruler and compared among DPS samples.

2.8.2. SEM

Three standard bacterial strains (*S aureus* (ATCC 25923), *E. coli* (ATCC 25922) and *P. aeruginosa* (PAO1)) grown on the DPS scaffolds were observed under SEM. For this purpose, 250 μl of bacterial suspensions (1.5×10^8 CFU/ml) were put on the DPS surfaces, and were incubated for 2 h at 37 °C. For taking images observed under SEM, the samples were washed with 1 ml PBS, and were fixed with 2.5% glutaraldehyde at room temperature for 2 h. The samples were further washed with PBS, and were dehydrated through a series of graded ethanol solutions (up to 100%). The samples were air-dried, sputter coated with gold and were observed under SEM (AIS2100; Seron Technology, Gyeonggi-do, South Korea).

2.9. Statistical analysis

All the data were analyzed by the GraphPad Prism v8.0.2.263 software using independent samples *t*-test and one-way ANOVA, where appropriate. The data were expressed as mean ± SD. A $P < 0.05$ was considered as the level of significance.

3. Results

3.1. Placenta characterizations

3.1.1. DNA content

The removal of the cells and nucleic acids from the ECM was confirmed by quantification of DNA content in the decellularized DPS samples. The DPS showed a significant decrease in DNA content after decellularization process when compared with the native placenta (Fig. 2, ****$P < 0.05$).

3.1.2. H&E staining

Staining was performed to further approve the removal of cells from the scaffolds. The placenta tissue before (control) and after decellularization processes (one, three and six months DPS samples) was stained with H&E and observed under light microscope (Fig. 3). The nuclei of

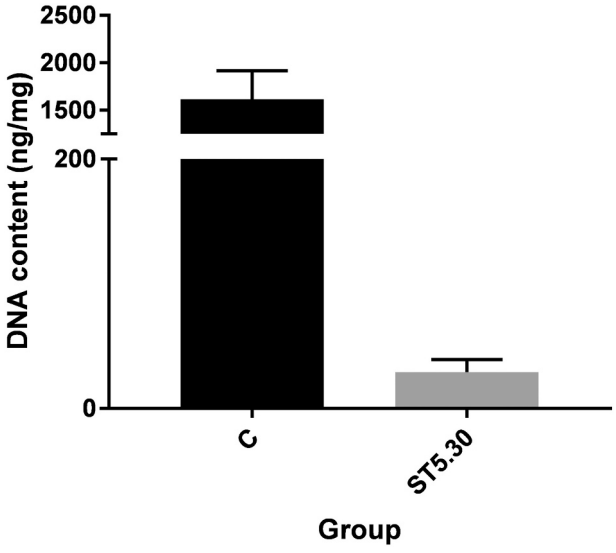

Fig. 2. Quantification of DNA content in native and decellularized placenta. Total DNA contents of ST 0.5/30 were less than 40 ng/mg of dry weight. Data are reported as the mean ± SD (****$P < 0.05$).

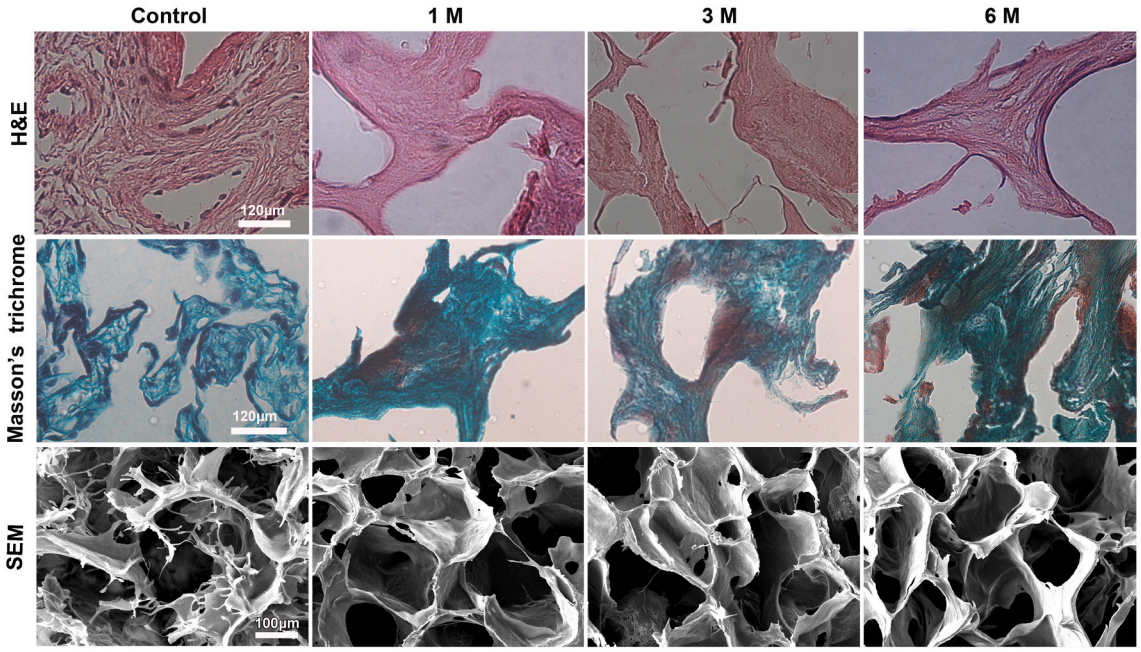

Fig. 3. H&E staining of the placenta sponge (control), and decellularized placental sponges after one, three and six months (1 M, 3 M and 6 M, respectively) storage. Yellow arrows indicate cell nuclei stained with hematoxylin. The collagen deposition (green) in placental sponges was visualized with Masson's trichrome (MT) staining. Microstructure morphology of the sponges was viewed under SEM. (For interpretation of the references to color in this figure legend, the reader is referred to the web version of this article.)

the cells counterstained with hematoxylin are shown with yellow arrows in the control samples. Histological observations of all the DPS tissues confirmed the successful removal of the cells or cells' fragments.

3.1.3. Masson's trichrome (MT) staining

This staining was designed to investigate the effects of decellularization and preservation time on the content of collagen in the ECM and its quality. The presence of collagen is an evidence of the intact ECM. The collagen in ECM of the placental sponges was stained with MT (stained in green) and was viewed under the light microscope (Fig. 3). The collagen fibers were observed in all the DPS samples. During the storage time up to six months a slightly decreased collagen content in DPS patches was observed. This was indicated by monitoring the decrease in green stained area and presence of red/brown stained area over time.

3.1.4. SEM

The DPS scaffolds were observed under SEM to compare their ultrastructural aspects with the control. SEM micrographs of the placental sponges are presented in Fig. 3. Control placental sponge showed the non-uniform microstructures, and non-continuous pore channels with very weak pores walls. All the DPS scaffolds exhibited a uniform microstructure with inter-connective networks.

3.2. In vitro cyto-biocompatibility assay

3.2.1. H&E staining

The DPS were cultured with Hu02 human foreskin fibroblasts for 7 days. Then, the samples were stained with H&E and observed under light microscope. The cells (yellow arrows) were grown well and proliferated within the pores of DPS in all samples with different storage times (Fig. 4a).

3.2.2. Cell viability

MTT assay showed that all the DPS had a good cytobiocompatibility with no changes in viability of Hu02 cells compared with control group (the cells cultured on plastic surface of cell culture plate) in all time intervals (Fig. 4b, $P > 0.05$).

3.2.3. SEM

The morphology of fibroblasts cultured for 7 days on DPS samples was observed under SEM, and the micrographs are shown in Fig. 4a. The cells were well attached and spread on all the DPSs, indicated with red arrows.

3.3. Angiogenesis assay

3.3.1. In vitro VEGF assay

The concentrations of VEGF in control placental sponge and DPS after keeping them at different storage times of one, three and six months were measured by ELISA assay. The decellularization process significantly reduced the VEGF content to around 160 ng/mg. However, six months preservation at −20 °C did not affect the VEGF concentrations in DPS samples.

3.3.2. In vivo angiogenesis assay

3.3.2.1. CAM assay. The potential of the DPS samples in promotion of new vessel formation around the DPS patches was evaluated by a CAM assay (Fig. 5a). The vessel percentage (Fig. 5b) and total vascular junction's number (Fig. 5c) were determined accordingly. No significant differences in vascular percentage were observed in all three DPS groups (one month = 40.88 ± 3.456, three months = 53.68 ± 3.999, and six months = 38.56 ± 3.545) (Fig. 5b). Vascular junction's number in six months DPS sample showed dramatic decrease as compared with one and three months DPS groups (739.0 ± 61.00 *vs* 322.5 ± 69.50, $P < 0/05$).

3.3.2.2. Histological evaluations (H&E and immunohistochemistry (IHC)). The H&E stained slides are shown in Fig. 6a. The cells and new vessels were observed within the DPS in three storage time intervals. To specifically stain the new vessel formation, the endothelial cells (CD31 positive cells) were visualized by IHC staining (Fig. 6b). After one and

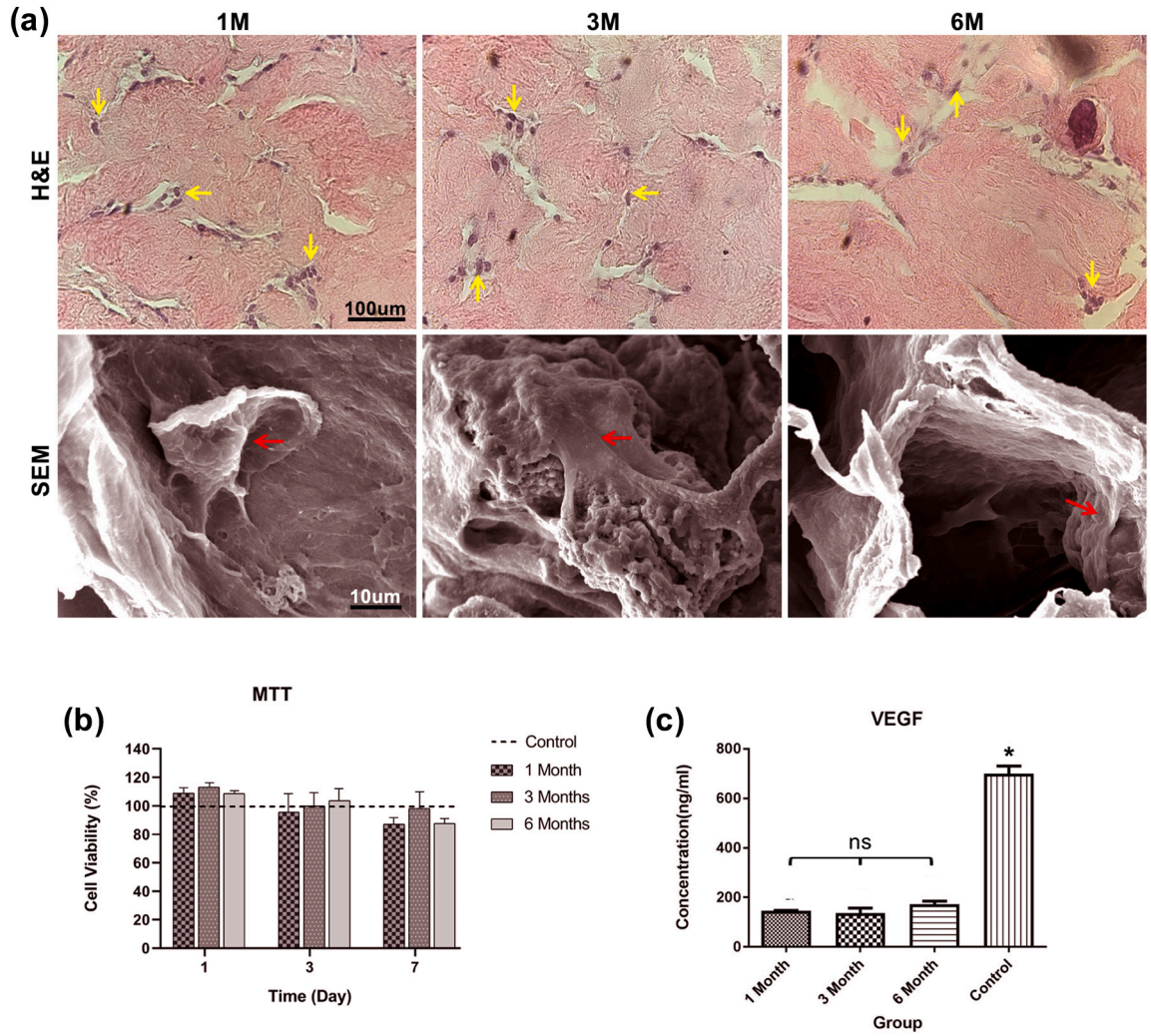

Fig. 4. (a) H&E staining of the decellularized placental sponges (DPS) cultured with Hu02 fibroblast cells. The cells were grown and were proliferated within the pores of sponges (yellow arrows). SEM micrographs of the cells (red arrows) cultured on the DPS. (b) The viability of the cells cultured on the DPS for different culture times of 1, 3 and 7 days, determined by MTT assay. (c) VEGF concentrations in the DPS tissues at different storage times in comparison with control placental sponge. Asterisk (*) and "ns" indicate significant and non-significant differences, respectively. (For interpretation of the references to color in this figure legend, the reader is referred to the web version of this article.)

four weeks post-implantation, the number of $CD31^+$ cells significantly decreased with the increase of storage time, as follows: one > three > six months (Fig. 6c).

3.4. *In vivo biocompatibility*

The $CD4^+$ (Fig. 7a) and $CD68^+$ (Fig. 7c) immune cells infiltrated into the implanted site after one and four weeks post-implantations were visualized with IHC staining to assess the presence of lymphocytes and macrophages as two main compartments of immune response, respectively. The number of $CD4^+$ cells at one and six weeks post-surgery showed a slight increase with the increase of storage time. Six-month samples had higher number of $CD4^+$ and $CD68^+$ positive cells infiltration as compared to one and three months samples. Nevertheless, only six-months samples at one-month post-implantation exhibited a significant increase in $CD4^+$ (Fig. 7b) and $CD68^+$ (Fig. 7d) positive cells as compared to other stored groups (one and three months) ($P < 0.05$).

3.5. *Antibacterial assays*

3.5.1. *Disk diffusion assay*

Disk diffusion results of one, three and six months stored DPSs for ATCC bacteria and MDR clinical isolates are shown in Fig. 8 to compare the ability of samples for bacterial growth inhibition. All the scaffolds (one, three and six months) showed an antibacterial activity against *S. aureus* standard strain (ATCC 25923). Nevertheless, the bacterial growth inhibition zone diameter decreased with the increase of storage time, as one-month DPS exhibited a larger growth inhibition zone than three and six months DPS for *S. aureus* ATCC 25923. Only one-month DPS had antibacterial activity against *E. coli* standard strain (ATCC 25922). *P. aeruginosa* standard strain (PAO1), and all MDR clinical isolates (*S. aureus* (MDR 50), *E. coli* (MDR 50), and *P. aeruginosa* (MDR 50)) revealed resistance to all DPS scaffolds.

3.5.2. *SEM*

SEM micrographs of the standard strain bacteria grown on DPS scaffolds are shown in Fig. 9. A few numbers of *S. aureus* standard strain (ATCC 25923) bacteria were observed in all the stored scaffolds (one, three and six months). *E. coli* standard strain (ATCC 25922) growth was observed only on three and six months DPS scaffolds, while *P. aeruginosa* standard strain (PAO1) bacteria were successfully grown on the all DPS scaffolds.

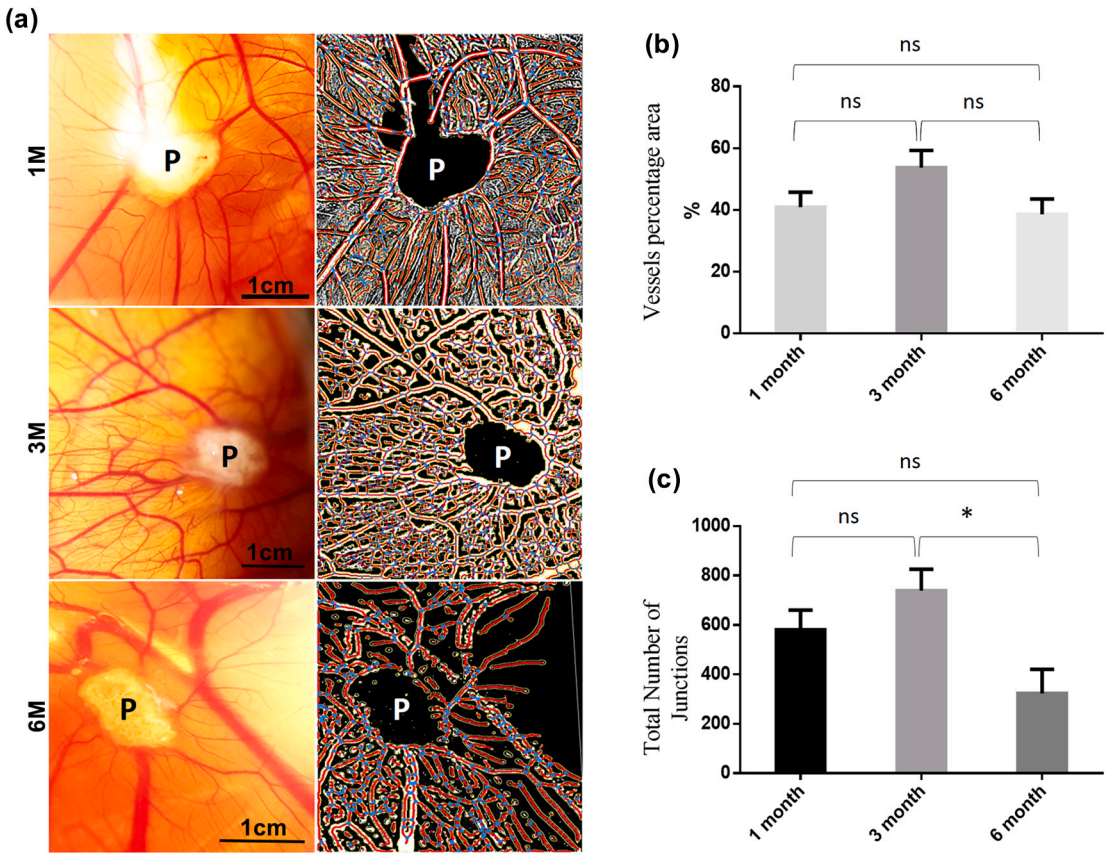

Fig. 5. (a) *In vivo* CAM assay; The decellularized placental sponges (P) samples were placed on the chick chorioallantoic membrane and the new vessel formation was observed and analyzed using stereomicroscope (left column) and ImageJ analysis (right column). (b) Vessel percentage area showed no significant difference between all the DPS groups. (c) A dramatic decrease in total vascular junction's number was observed in six months stored DPS when compared with one and three months samples. Asterisk (*) and "ns" indicate significant and non-significant differences, respectively.

4. Discussion

The application of human placenta and its derivatives has been one of the major objectives in several studies in regenerative medicine [27]. Some of examples like the use of placenta-derived allografts in bullous keratopathy, plantar fasciitis and diabetic foot ulcers have reached clinical stages [28–30]. Stimulation of host immune response and rejection are the most important remaining challenges in allogeneic- and xenogeneic-derived scaffolds. A possible solution of this problem is the complete removal of the cells from the tissue, known as decellularization process [13,31]. This process can negatively influence the biomechanical and biophysical properties of the tissues. Therefore, different decellularization protocols have been developed to fabricate an acellular scaffold/sponge/matrix with minimal negative effects on the ECM component and biomechanical properties [5,22].

In our study, we determined the effects of decellularization process and storage duration (one, three and six months) on angiogenic and antibacterial properties of the fabricated decellularized placental sponge (DPS). After decellularization of placenta with ionic detergent (SDS), the removal of the cells was confirmed by H&E staining. The cell nuclei stained with hematoxylin were observed in control group (without application of decellularization method), while there was no trace of cell nuclei in the decellularized tissue. Mason's trichrome (MT) staining results revealed a well-preserved collagen content without any trace of cell nuclei in all the experimental scaffolds, implicating minimal disruption of ECM after decellularization and storage period. This outcome was previously confirmed by Flynn et al. [5]. SDS is an ionic detergent, which is extensively used in the decellularization of tissues [32]. Despite being very efficient on removing cells, some reports highlighted the detrimental effects of SDS such as damages to tissue ECM, and biomechanical and biochemical changes on the treated tissues [33–35]. Although SDS can be harmful to some structural and signal proteins, other studies demonstrated its effectiveness on complete cell removal without damaging the biocompatibility properties of the tissues [36,37]. The morphological investigations of all experimental groups under SEM exhibited a uniform structure with interconnected channels in all DPS samples in comparison with deformed microstructure with low uniformity, and disconnected pore channels of the control group (non decellularized placental membrane scaffolds/sponges).

In vitro biocompatibility of the DPS scaffolds was determined by MTT assay and histological observations, further confirmed by SEM. The H&E staining of Hu02 human foreskin fibroblast cells cultured on DPSs for 7 days revealed good distribution and growth of the cells within the porous channels of all three experimental sponges. The MTT assay demonstrated that a storage period of DPS up to six months did not affect the viability of the fibroblasts grown on the stored DPS scaffolds for 1, 3 and 7 days. The excellent cell adhesion and distribution were observed under SEM. Some investigators [38–40] reported the biocompatibility of the placenta-derived scaffolds for human foreskin fibroblasts, human epidermal keratinocytes, human amniotic membrane-derived stem cells [3] and mesenchymal cells [40].

As stated earlier, the placenta tissue contains several pro-angiogenic factors such as VEGF and bFGF [23]. Additionally, placenta-derived wound dressings showed to improve neovascularization and wound healing, and are considered as an excellent candidate for skin tissue engineering applications. Rameshbabu et al. [3], designed a sponge using placental ECM and silk fibroin to promote full-thickness cutaneous wound healing through neovascularization and cell migration. They

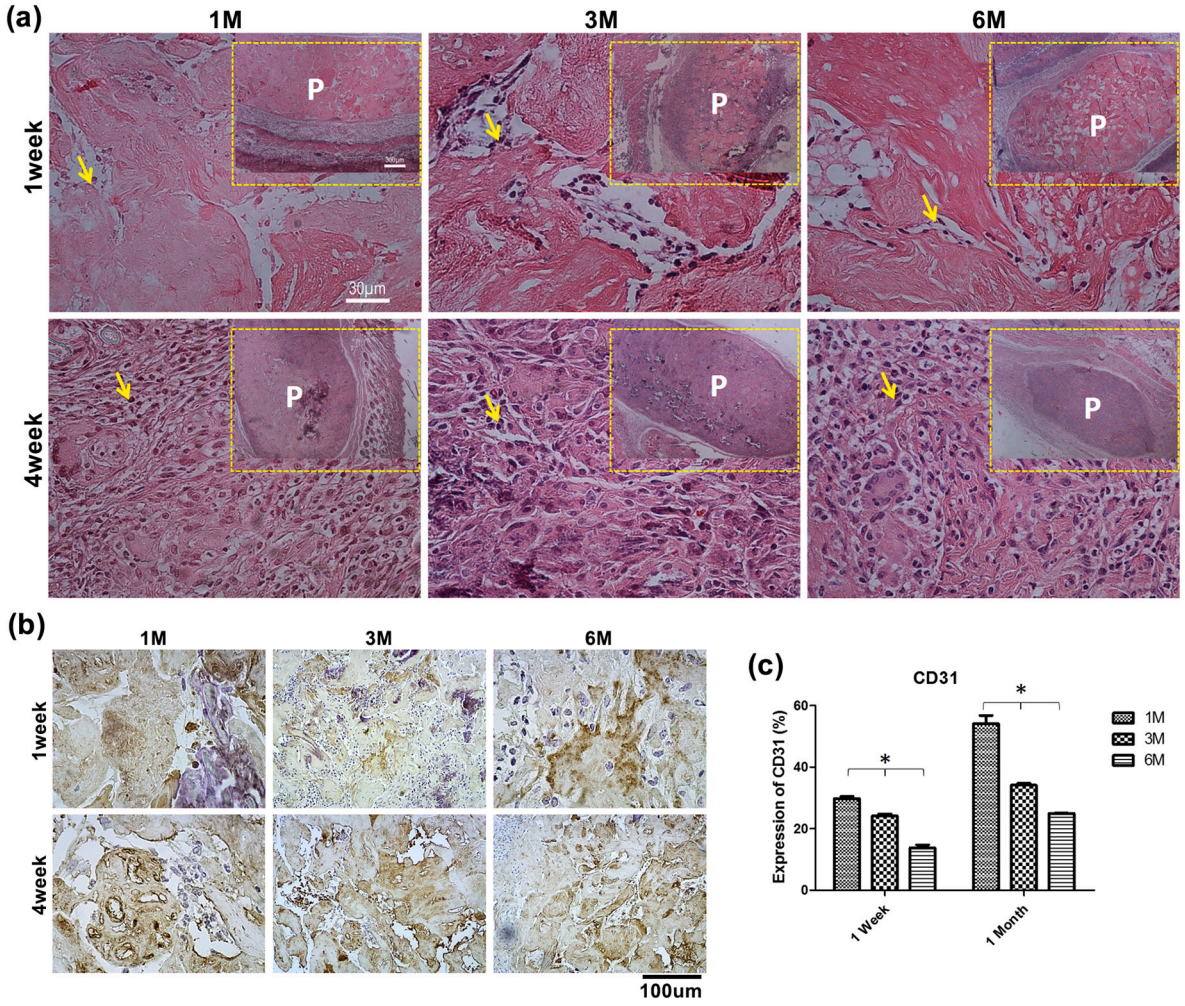

Fig. 6. (a) H&E staining of the slides. Inserted yellow dash lines show low magnification image. (b) IHC staining of CD31 positive cells for one, three and six months DPS groups after one and four weeks of subcutaneous implantation. (c) The comparison of CD31 positive cells' numbers between the experimental groups after one and four weeks of subcutaneous implantation. Asterisk (*) and ns indicate significant and insignificant differences, respectively. (For interpretation of the references to color in this figure legend, the reader is referred to the web version of this article.)

observed a superior neovascularization and accelerated re-epithelialization without the formation of scar in their hybrid extracellular matrix sponge group as compared to other experimental groups. The implanted wounds showed an increased expression of endogenous factors like IGF-1, VEGFA, HGF, PDGF-B and others. In our previous work, we designed and fabricated a placental-derived amniotic membrane and silk fibroin bilayer scaffolds to improve the scarless wound healing in two wounds models of full-thickness wounds in a mouse and a rabbit ear model. We observed an accelerated angiogenesis, ECM remodeling and wound healing without scar formation [25,41,42].

The measurement of VEGF concentrations in DPS samples by ELISA revealed a significant reduction of VEGF content after decellularization process. This decrease is more likely due to treatment of tissue with SDS during the decellularization process, as confirmed by Xing et al. [34]. The decrease in growth factor concentration after decellularization with SDS was also reported [8,13,43]. In this regards, Choi and coworkers showed that the treatment of placental tissue with SDS significantly decrease the growth factors contents after decellularization process [36]. We showed in this work that there was no significant difference in VEGF content among the stored DPS scaffolds for one, three and six months. This suggests that the storage time up to six months has no considerable effect on VEGF concentration in DPSs. Chick chorioallantoic membrane (CAM) assay was performed to evaluate the effects of storage time on the *in vivo* angiogenic capacity of the decellularized sponges. There was no difference between the blood vessel percentage areas among all DPS samples with different storage times. However, the total number of vascular junctions drastically decreased in six months stored DPS sample as compared to one and three months stored DPS samples. This suggests that the angiogenic property of the decellularized sponges depends on the storage time, as decreases with the increase of storage time. Long-term changes and damages to the *in vitro* preserved tissues were also reported by Baiguera et al. [44]. The DPS samples (1, 3 and 6 M) were implanted subcutaneously in mice, and were studied after one and four weeks post-implantation for their angiogenic properties and biocompatibility *in vivo*. The IHC staining of CD31 revealed that the number of CD31 positive cells significantly decreased with the increase of storage time. One and six months DPS samples showed highest and lowest density of $CD31^{+}$ cells in both one and four weeks post-implantation time points. CD31 is a transmembrane homophilic receptor that is abundantly expressed in the junctions of endothelial cells [45]. Endothelial cells can easily switch to angiogenesis when needed [46]. Our findings show that the angiogenic property of the DPS patches decreases over the preservation time from one to six months. Our *in vivo* IHC data on new vessel formation was consistent with the results obtained from CAM assay.

The biocompatibility of tissue engineering scaffolds/sponges is crucial for their functions in biomedical approaches [47]. Body's immune response is the first host reaction to the implanted biomaterials

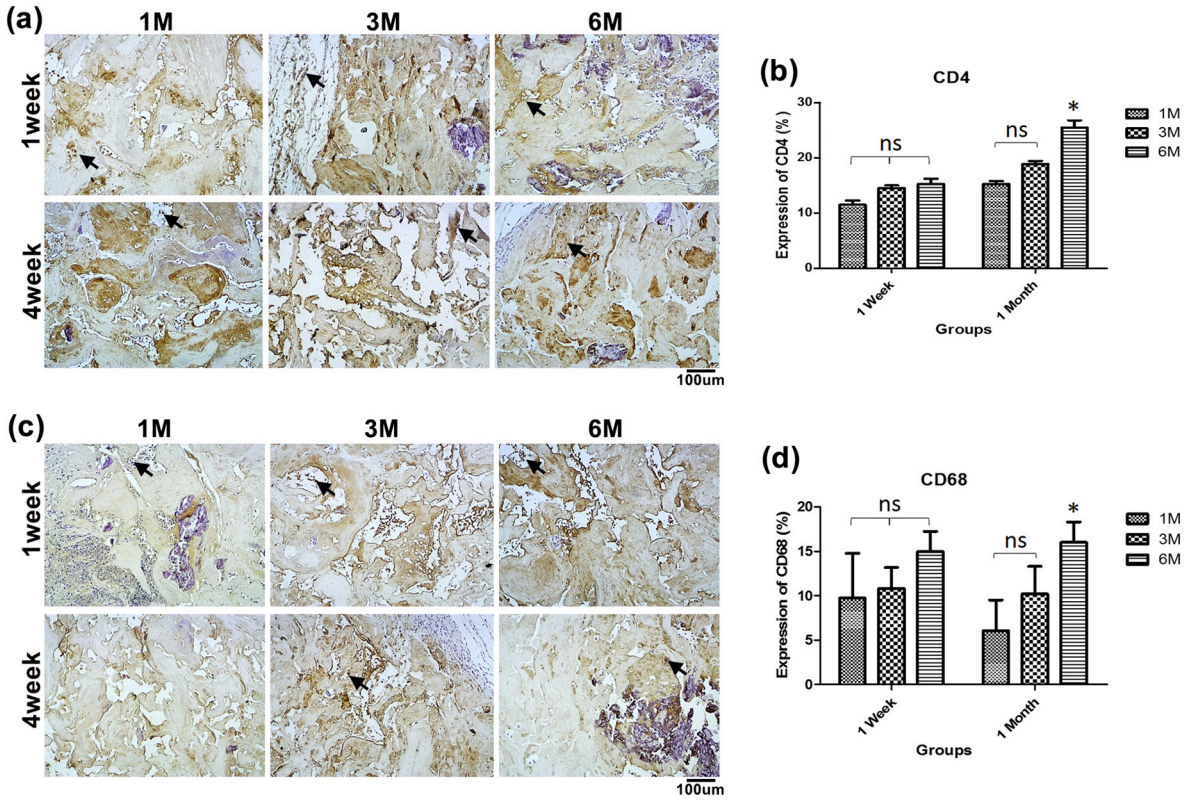

Fig. 7. IHC staining of $CD4^+$ (a and b) and $CD68^+$ (c and d) positive cells in the skin tissue subcutaneously implanted with one, three and six months scaffolds at one and four weeks post-implantation. The number of $CD4^+$ and $CD68^+$ cells in six-months scaffold after four weeks subcutaneous implantation showed a significant increase compared with other scaffolds ($P < 0.05$). Black arrow indicates positive cells.

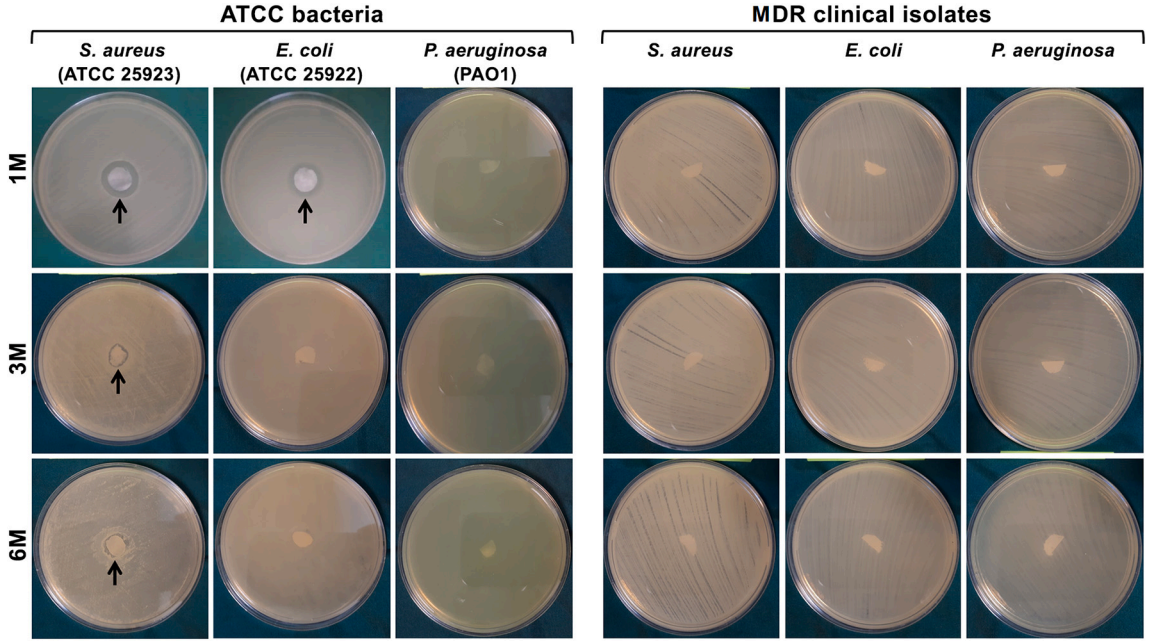

Fig. 8. Disk diffusion assay for one, three and six months stored decellularized placental sponges (DPS) scaffolds against standard strains and MDR clinical isolates. Black arrows indicate growth inhibition zone around the DPS disk.

[48]. To examine the effects of decellularization method and storage duration on the biocompatibility of DPSs *in vivo*, the infiltration of $CD4^+$ and $CD68^+$ positive cells was determined by IHC staining. CD4 and CD68 represent lymphocyte and macrophage, respectively [49]. $CD4^+$ T lymphocyte cells play a critical role in regulating immune responses, and mediate several functions related to innate and adaptive immune systems [50]. CD68 is highly expressed by macrophages and is considered as a reliable candidate for identification of these cells [51]. IHC results indicated that the storage period did not affect the infiltration rate of CD4 and CD68 positive cells after one week of implantation. On week

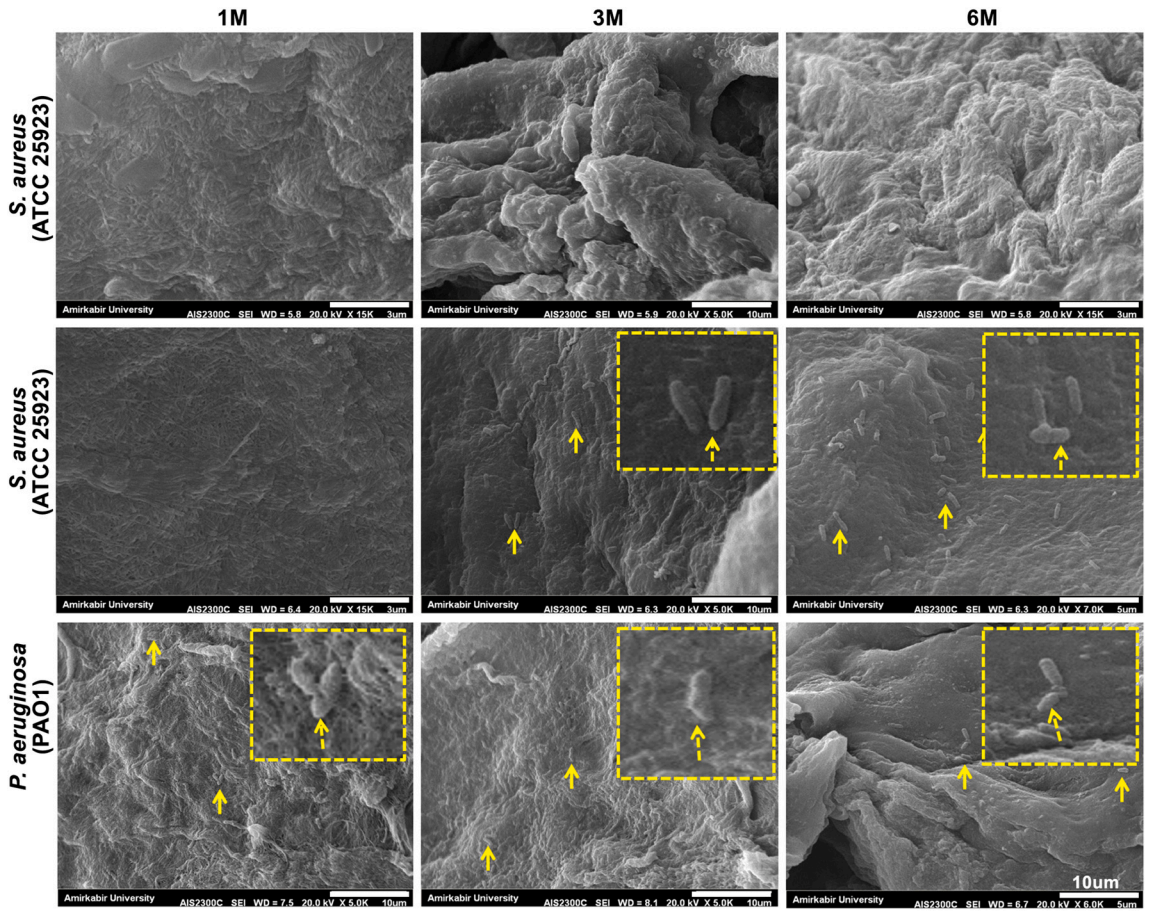

Fig. 9. SEM micrographs of show the growth of standard strain bacteria on one, three and six months stored decellularized placental sponge scaffolds. Yellow arrows indicate the bacteria grown on the different scaffolds. The grown bacteria are clearly seen in the inserted images with higher magnification. (For interpretation of the references to color in this figure legend, the reader is referred to the web version of this article.)

four, however, the six months stored DPS showed a significant increase in the number of $CD4^+$ and $CD68^+$ cells when compared with one and three months DPS samples.

Within the first few hours after implantation of a medical device, tissue and blood macrophages play a key role in body's immune response to these devices. Afterwards, T_H lymphocytes mediate the polarization of macrophages from pro-inflammatory phase to pro-healing. If this switching fails by the activity of a low-biocompatible biomaterial, this inflammation leads to fibrosis [52].

Wilshaw et al. [53] reported that their SDS-treated acellular placenta-derived amniotic membrane demonstrated a low level of T-cells and high numbers of macrophages after three months subcutaneous implantation in mice compared with native and glutaraldehyde-treated amniotic membrane. They found that the implanted tissue was in the process of remodeling rather than being rejected. Xu et al. [54] transplanted a human decellularized dermal matrix in the abdominal wall of a primate model and reported a mild response of macrophages and T-cells at the first month post-surgery, and eliminated after six months follow-up. These results are consistent with those reported by Bonenfant et al. [55]. They found that the different storage times and sterilization procedures can affect the protein content of the decellularized lung. Therefore, the prepared materials should not be stored more than three months.

The ECM of placenta compartments such as amniotic membrane contains several antimicrobial agents such as β-defensins, secretory leukocyte proteinase inhibitor (SLPI) and elafin [10,38,56]. The effects of storage period on antibacterial properties of the DPS scaffolds against three standard bacterial strains and three MDR bacteria were evaluated by disk diffusion method and were observed under SEM. All the DPS scaffolds exhibited a strong antibacterial activity against *S. aureus* standard strain. The disk diffusion assay revealed a decrease in the diameter of growth inhibition zone of *S. aureus* with the increase of storage duration. In addition, only one month DPS inhibited the growth of *E. coli* standard strain, while three and six months DPS stored samples revealed no growth inhibition zone for *E. coli*. *P. aeruginosa* standard strain and all the MDR strains of bacteria were resistant to all DPS scaffolds/sponges. It is observed that the antibacterial activity of the DPS is time-dependent, and is decreased over time. The results obtained from the antibacterial assays indicated that the antibacterial behavior of the DPS also depends on the strain of bacteria, and has no protection potential against resistant bacteria.

Tehrani et al. [20] evaluated the effects of preservation methods (cryopreservation and freeze-drying) on antibacterial property of the amniotic membrane. The amniotic membrane showed antibacterial behavior against *P. aeruginosa* ATCC 27853 and 2 clinically isolates of *E. coli*, and no antimicrobial activity for *S. aureus* ATCC 25923 and *E. coli* ATCC 25922. According to their results, cryopreservation and freeze-drying preservation methods did not affect the antibacterial property of the amniotic membrane. In our recent investigation, we showed that the antibacterial properties of decellularized amniotic membrane depend on the bacterial strain. The decellularized amniotic membrane had a strong antibacterial activity against three standard strains of *Escherichia coli* (ATCC 25922), *Pseudomonas aeruginosa* (ATCC 27833), and *S. aureus* (ATCC 25923) bacteria, while no antibacterial behavior against clinical isolates was observed. We also revealed that decellularization did not affect the antibacterial activity of the amniotic

membrane [38]. In the current study, we revealed that the biocompatibility, angiogenic and antibacterial properties of the decellularized placenta fabricated scaffolds/sponges are significantly altered over duration of storage time.

5. Conclusion

Decellularization, preservation and storage period influence the biomechanical and biological properties of allografts and xenografts. All the decellularized placental sponge samples here tested have no antibacterial activity against resistant clinical isolates, independent to storage time. Antibacterial activity of the sponges against standard strains depends on bacterial strains and is also affected by preservation time. According to our *in vitro* and *in vivo* observations, angiogenic properties and biocompatibility of the sponges are also significantly affected by storage time, since six months preserved sponges showed a higher number of lymphocytes infiltrated into the implanted site, and decreased angiogenesis factors and new vessel formation compared to one and three months storage. Three months preservation at −20 °C is suggested as the optimal storage period to retain its biocompatibility, angiogenic properties and antibacterial activity. The results obtained from this investigation may be considered for preservation of biological-based tissue engineering products like decellularized placental sponge patches with the aim of retaining their specific biological properties.

CRediT authorship contribution statement

MG and SCK conceived and designed the study. FA, SK, MK, AH, ZAA, HGH and AS performed the experiments. MG, MK and NPS analyzed the data and interpreted the results. FA, SK, ZAA, HGH and AS prepared the manuscript. MG, SCK, LM and RLS reviewed during the preparation of manuscript and revised the manuscript.

Declaration of competing interest

The authors declare that they have no known competing financial interests or personal relationships that could have appeared to influence the work reported in this paper.

Acknowledgements

This study was supported by Iran University of Medical Sciences (grant no; 15535) and Iran National Science Foundation (INSF, 98022911). SCK presently holds European Research Area Chair and Full Professor position at 3Bs Research Group, University of Minho, Portugal supported by the European Union Framework Programme for Research and Innovation HORIZON 2020 under grant agreement no. 668983 - FoReCaST.

References

[1] S. Heydarkhan-Hagvall, K. Schenke-Layland, A.P. Dhanasopon, F. Rofail, H. Smith, B.M. Wu, R. Shemin, R.E. Beygui, W.R. MacLellan, Biomaterials 29 (2008) 2907–2914.
[2] J.M. Aamodt, D.W. Grainger, Biomaterials 86 (2016) 68–82.
[3] A.P. Rameshbabu, K. Bankoti, S. Datta, E. Subramani, A. Apoorva, P. Ghosh, P. P. Maity, P. Manchikanti, K. Chaudhury, S. Dhara, ACS Appl. Mater. Interfaces 10 (2018) 16977–16991.
[4] T. Hoshiba, H. Lu, N. Kawazoe, G. Chen, Expert. Opin. Biol. Ther. 10 (2010) 1717–1728.
[5] L. Flynn, J.L. Semple, K.A. Woodhouse, J. Biomed. Mater. Res. A 79 (2006) 359–369.
[6] K.H. Schneider, P. Aigner, W. Holnthoner, X. Monforte, S. Nürnberger, D. Rünzler, H. Redl, A.H. Teuschl, Acta Biomater. 29 (2016) 125–134.
[7] J.P. Alves-Lopes, J.-B. Stukenborg, Hum. Reprod. Update 24 (2018) 176–191.
[8] S. Khosravimelal, M. Momeni, M. Gholipur, S.C. Kundu, M. Gholipourmalekabadi, (2019).
[9] G.d.S.S. Matias, N.N. Rigoglio, A.C.O. Carreira, P. Romagnolli, R.d.S.N. Barreto, A. M. Mess, M.A. Miglino, P. Fratini, Cells Tissues Organs, 205 (2018) 217–225.
[10] A.K. Riau, R.W. Beuerman, L.S. Lim, J.S. Mehta, Biomaterials 31 (2010) 216–225.
[11] L.C.P.C. Leonel, C. Miranda, T. Coelho, G. Ferreira, R. Caãada, M. Miglino, S. Lobo, Brazilian Journal of Medical and Biological Research, 51, 2018.
[12] A. Gilpin, Y. Yang, Biomed. Res. Int. 2017 (2017) 9831534.
[13] P.M. Crapo, T.W. Gilbert, S.F. Badylak, Biomaterials 32 (2011) 3233–3243.
[14] E. Díaz-Moreno, D. Durand-Herrera, V. Carriel, M.Á. Martín-Piedra, M.d.C. Sánchez-Quevedo, I. Garzón, A. Campos, R. Fernández-Valadés, M. Alaminos, Journal of Biomedical Materials Research Part B: Applied Biomaterials, 106 (2018) 488–500.
[15] W.F. Wolkers, A. Hilfiker, Freeze-drying of Decellularized Heart Valve Tissues, Springer, Cryopreservation and Freeze-drying Protocols, 2015, pp. 499–506.
[16] S. Zouhair, P. Aguiari, L. Iop, A. Vásquez-Rivera, A. Filippi, F. Romanato, S. Korossis, W.F. Wolkers, G. Gerosa, Acta Biomater. 84 (2019) 208–221.
[17] A. Johnson, A. Gyurdieva, S. Dhall, A. Danilkovitch, Y. Duan-Arnold, Ann. Plast. Surg. 79 (2017) 203–213.
[18] H. Niknejad, T. Deihim, M. Solati-Hashjin, H. Peirovi, Cryobiology 63 (2011) 145–151.
[19] M.T. Rodríguez-Ares, M.J. López-Valladares, R. Touriño, B. Vieites, F. Gude, M. T. Silva, J. Couceiro, Acta Ophthalmol. 87 (2009) 396–403.
[20] F.A. Tehrani, A. Ahmadiani, H. Niknejad, Cryobiology 67 (2013) 293–298.
[21] Z. Kakabadze, A. Kakabadze, D. Chakhunashvili, L. Karalashvili, E. Berishvili, Y. Sharma, S. Gupta, Hepatology 67 (2018) 1956–1969.
[22] J.S. Choi, J.D. Kim, H.S. Yoon, Y.W. Cho, Tissue Eng. A 19 (2013) 329–339.
[23] K. Forbes, M. Westwood, J. Endocrinol. 207 (2010) 1–16.
[24] G.A.o.t.W.M. Association, The Journal of the American College of Dentists, 81 (2014) 14.
[25] M. Gholipourmalekabadi, S. Khosravimelal, Z. Nokhbedehghan, M. Sameni, V. Jajarmi, A.M. Urbanska, H. Mirzaei, M. Salimi, N.P.S. Chauhan, M. Mobaraki, et al., ACS Biomater. Sci. Eng. 5 (2019) 1487–1496.
[26] P.-R. Hsueh, W.-C. Ko, J.-J. Wu, J.-J. Lu, F.-D. Wang, H.-Y. Wu, T.-L. Wu, L.-J. Teng, Journal of microbiology, Immunol. Infect. 43 (2010) 452–455.
[27] A.R. Silini, A. Cargnoni, M. Magatti, S. Pianta, O. Parolini, Frontiers in Bioengineering and Biotechnology, 3 (2015) 162.
[28] L. Venegas, M. Hettich, J. Villena, R. Aris, M. Párraga, O. Parolini, M. Alaminos, A. Campos, S. San Martin, J. Stem Cell Res. Ther. 4 (2014) 4172.
[29] C.M. Zelen, A. Poka, J. Andrews, Foot Ankle Int. 34 (2013) 1332–1339.
[30] C.M. Zelen, T.E. Serena, R.J. Snyder, Int. Wound J. 11 (2014) 122–128.
[31] M. Gholipourmalekabadi, M. Mozafari, M. Salehi, A. Seifalian, M. Bandehpour, H. Ghanbarian, A.M. Urbanska, M. Sameni, A. Samadikuchaksaraei, A.M. Seifalian, Adv. Healthc. Mater. 4 (2015) 918–926.
[32] M. Alizadeh, L. Rezakhani, M. Soleimannejad, E. Sharifi, M. Anjomshoa, A. Alizadeh, Heliyon 5 (2019), e02253.
[33] J.D. O'Neill, R. Anfang, A. Anandappa, J. Costa, J. Javidfar, H.M. Wobma, G. Singh, D.O. Freytes, M.D. Bacchetta, J.R. Sonett, Ann. Thorac. Surg. 96 (2013) 1046–1056.
[34] Q. Xing, K. Yates, M. Tahtinen, E. Shearier, Z. Qian, F. Zhao, Tissue Eng. C Methods 21 (2015) 77–87.
[35] J. Zhou, O. Fritze, M. Schleicher, H.-P. Wendel, K. Schenke-Layland, C. Harasztosi, S. Hu, U.A. Stock, Biomaterials 31 (2010) 2549–2554.
[36] J.P. Guyette, J.M. Charest, R.W. Mills, B.J. Jank, P.T. Moser, S.E. Gilpin, J. R. Gershlak, T. Okamoto, G. Gonzalez, D.J. Milan, G.R. Gaudette, H.C. Ott, Circ. Res. 118 (2016) 56–72.
[37] J. Fernández-Pérez, M. Ahearne, Sci. Rep. 9 (2019) 14933.
[38] M. Gholipourmalekabadi, M. Bandehpour, M. Mozafari, A. Hashemi, H. Ghanbarian, M. Sameni, M. Salimi, M. Gholami, A. Samadikuchaksaraei, Burns 41 (2015) 1488–1497.
[39] M. Gholipourmalekabadi, M. Sameni, D. Radenkovic, M. Mozafari, M. Mossahebi-Mohammadi, A. Seifalian, Cell Prolif. 49 (2016) 115–121.
[40] Ö.S. Somuncu, Y. Coşkun, B. Ballica, A.F. Temiz, D. Somuncu, J. Clin. Neurosci. 59 (2019) 291–297.
[41] M. Gholipourmalekabadi, A. Samadikuchaksaraei, A.M. Seifalian, A.M. Urbanska, H. Ghanbarian, J.G. Hardy, M.D. Omrani, M. Mozafari, R.L. Reis, S.C. Kundu, Biomed. Mater. 13 (2018), 035003.
[42] M. Gholipourmalekabadi, A.M. Seifalian, A.M. Urbanska, M.D. Omrani, J.G. Hardy, Z. Madjd, S.M. Hashemi, H. Ghanbarian, P. Brouki Milan, M. Mozafari, Biomacromolecules 19 (2018) 2409–2422.
[43] J.E. Reing, B.N. Brown, K.A. Daly, J.M. Freund, T.W. Gilbert, S.X. Hsiong, A. Huber, K.E. Kullas, S. Tottey, M.T. Wolf, S.F. Badylak, Biomaterials 31 (2010) 8626–8633.
[44] S. Baiguera, C. Del Gaudio, M.O. Jaus, L. Polizzi, A. Gonfiotti, C.E. Comin, A. Bianco, D. Ribatti, D.A. Taylor, P. Macchiarini, Biomaterials 33 (2012) 3662–3672.
[45] P. Lertkiatmongkol, D. Liao, H. Mei, Y. Hu, P.J. Newman, Curr. Opin. Hematol. 23 (2016) 253–259.
[46] K. De Bock, M. Georgiadou, P. Carmeliet, Cell Metab. 18 (2013) 634–647.
[47] L. Chung, D.R. Maestas Jr., F. Housseau, J.H. Elisseeff, Adv. Drug Deliv. Rev. 114 (2017) 184–192.
[48] K. Sadtler, M.T. Wolf, S. Ganguly, C.A. Moad, L. Chung, S. Majumdar, F. Housseau, D.M. Pardoll, J.H. Elisseeff, Biomaterials 192 (2019) 405–415.
[49] L. Wang, J.A. Johnson, Q. Zhang, E.K. Beahm, Acta Biomater. 9 (2013) 8921–8931.
[50] R.V. Luckheeram, R. Zhou, A.D. Verma, B. Xia, Clinical and Developmental Immunology, 2012, 2012.
[51] D.A. Chistiakov, M.C. Killingsworth, V.A. Myasoedova, A.N. Orekhov, Y. V. Bobryshev, Lab. Investig. 97 (2017) 4–13.
[52] A. Vishwakarma, N.S. Bhise, M.B. Evangelista, J. Rouwkema, M.R. Dokmeci, A. M. Ghaemmaghami, N.E. Vrana, A. Khademhosseini, Trends Biotechnol. 34 (2016) 470–482.

[53] S.-P. Wilshaw, J. Kearney, J. Fisher, E. Ingham, Tissue Eng. A 14 (2008) 463–472.
[54] H. Xu, H. Wan, M. Sandor, S. Qi, F. Ervin, J.R. Harper, R.P. Silverman, D. J. McQuillan, Tissue Eng. A 14 (2008) 2009–2019.
[55] N.R. Bonenfant, D. Sokocevic, D.E. Wagner, Z.D. Borg, M.J. Lathrop, Y.W. Lam, B. Deng, M.J. DeSarno, T. Ashikaga, R. Loi, Biomaterials 34 (2013) 3231–3245.
[56] M. Gholipourmalekabadi, B. Farhadihosseinabadi, M. Faraji, M.R. Nourani, Burns 46 (2019) 1254–1271.